ISSN 1054-660X, Laser Physics, 2007, Vol. 17, No. 8, pp. 1029–1032.

Compact Eye-Safe Intracavity Optical Parametric Oscillator with Efficient Pulse Shortening

J. G. Miao[a, b], B. S. Wang[a, b], J. Y. Peng[a, b], H. K. Bian[a, b], and H. M. Tan[a]

[a] *Changchun Institute of Optics, Fine Mechanics, and Physics, Chinese Academy of Sciences, Changchun Jilin, 130033 China*

[b] *Graduate School of the Chinese Academy of Sciences, Beijing, 100039 China*

e-mail: mjgbhk@yahoo.com

Received October 16, 2006

Abstract—We report a compact eye-safe intracavity optical parametric oscillator (IOPO), driven by a diode end-pumped passively Q-switched $Nd:YVO_4$/Cr:YAG laser. At the incident diode pump power of 6.2 W and signal pulse repetition rate of 13 kHz, we obtain a minimum signal pulse duration as short as 1.3 ns, holding a pulse compressing factor of 17 with respect to that of the pump, and exhibiting an efficient pulse shortening mechanism. At the same time, the maximum average power of 110 mW and pulse energy of 8.5 μJ for the signal wave are also achieved. In addition, cavity dumping characteristics and the correlation dynamics between the laser and the OPO are qualitatively analyzed.

PACS numbers: 42.55.Xi, 42.60.Gd, 42.65.Yj, 42.65.Re

DOI: 10.1134/S1054660X07080014

1. INTRODUCTION

Compact all-solid-state eye-safe laser sources, emitting around 1.5 μm, with a high repetition rate and narrow pulse width, have proven attractive in applications such as laser radar, remote sensing, etc. [1, 2]. Eye-safe radiation can be achieved by erbium-doped lasers, stimulated Raman scattering (SRS), or by noncritically phase-matched (NCPM) KTP-based intracavity optical parametric oscillators (IOPOs). To our knowledge, erbium eye-safe lasers usually exhibit a low pulse repetition rate and peak power, which restrict their practical use. The main drawback of SRS lasers, based on the first or third Stokes' shift, is their high resonating threshold and low optical conversion efficiency [3]. Currently, all-solid-state self-SRS can directly shift 1.34 to 1.54 μm eye-safe radiation, with compact configuration and relatively high efficiency [4]. However, sufficiently high intensity of 1.34 μm is very difficult to obtain, since the effective emission cross section at this laser line is very small due to the parasitic excited state absorption (ESA) loss [5]. Owing to their high efficiency and relatively low threshold, NCPM–KTP–IOPOs are considered as potentially promising eye-safe laser sources in the near future.

Taking advantage of the intense intracavity power in the pump laser, IOPO reduces the pump level necessary to exceed the oscillation threshold and increases the overall efficiency. In fact, IOPO serves as a nonlinear cavity dumper to extract the energy stored in the intracavity optical field, resulting in a significant pulse shortening mechanism. Since the early 1990s, IOPO has gained a renaissance after about 20 years of dreariness. Nevertheless, the pump sources mainly are flashlamp side-pumped or quasi-cw-diode end-pumped, actively Q-switched lasers [6, 7], with a low pulse repetition rate and low overall efficiency. In recent years, cw-diode end-pumped all-solid-state Cr:YAG passively Q-switched lasers, with the merits of a low cost, high efficiency, compactness, and simplicity [8, 9], have attracted a great deal of attention and become an alternative to actively Q-switched lasers. Furthermore, the typically used active medium for IOPO operation is mostly focused on Nd:YAG crystals with unpolarized emission due to its intrinsical isotropy. Therefore, a polarizer is often required in order to enhance the parametric conversion efficiency, which inevitably brings additional inserting loss into the cavity. Compared with Nd:YAG, $Nd:YVO_4$ crystals have a higher absorption cross section, wider gain bandwidth, and a particularly linear polarized output. As a result, $Nd:YVO_4$ has proven to be an ideal medium for nonlinear frequency conversion and diode end-pumped all-solid-state lasers.

In this letter, we report a compact eye-safe IOPO, emitting at 1573 nm, with a diode end-pumped passively Q-switched $Nd:YVO_4$/Cr:YAG laser. At the incident pump power of 6.2 W and signal pulse repetition rate of 13 kHz, we get a minimum signal pulse width of 1.3 ns, with a pulse-shortening factor of 17 to the pump pulse. To our knowledge, this is a very efficient pulse-shortening phenomenon. At the same time, the maximum average power of 110 mW and pulse energy of 8.5 μJ for the signal wave are also obtained.

2. EXPERIMENTAL SETUP

The schematic experimental setup is shown in Fig. 1. A plane-concave cavity configuration is employed, and the KTP crystal is placed near the output

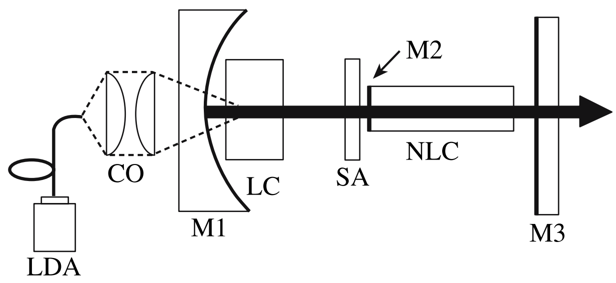

Fig. 1. Experimental setup of the IOPO system: LDA, laser diode array; CO, coupling optics; M1, input mirror; LC, laser crystal; SA, Cr:YAG saturable absorber; NLC, KTP crystal; M3, output coupler.

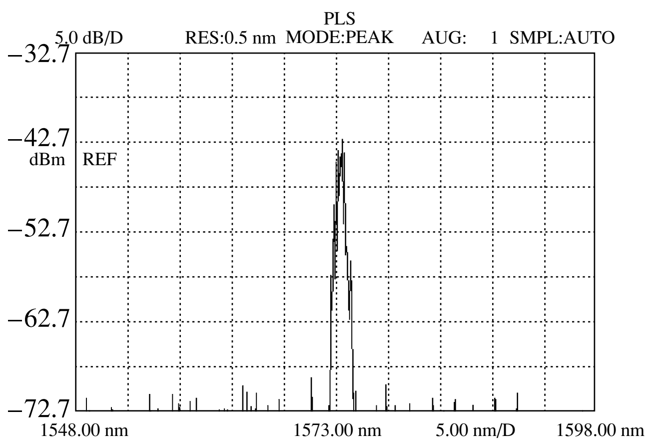

Fig. 2. Typical spectrum of the signal wave, with a center wavelength of 1573.3 nm.

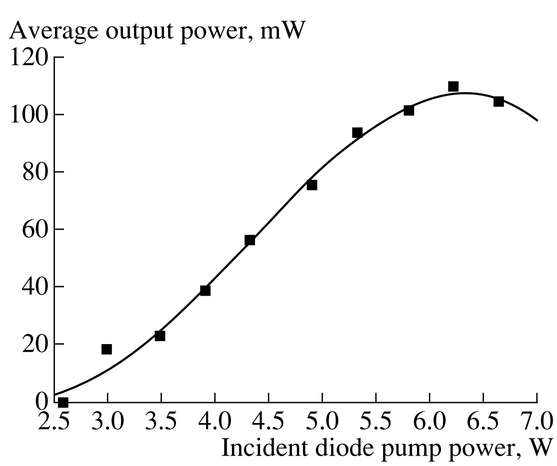

Fig. 3. Average output power at 1573 nm, with respect to the incident diode pump power.

coupler, where the pump spot is small enough to give the highest parametric gain and the lowest pump threshold. The pump source is driven by a fiber-coupled cw diode array (LIMO Co., Germany), emitting at 808 nm (at room temperature), with a maximum output power of 20 W. And, the pump beam is focused into the laser crystal by collimating and focusing lens pairs, whose focal length is 23 mm, with a beam waist around 200 μm. As the active medium, the $3 \times 3 \times 2$ mm^3, a-cut 1.0 at. % doped Nd:YVO_4 crystal is antireflection (AR) coated at 1064 nm on both sides. The Cr:YAG saturable absorber, with an initial transmission of 83% and a thickness of 1.8 mm, is also AR coated at 1064 nm. A 20 mm long, type-II noncritically phase-matched KTP crystal is used as the nonlinear converter. Furthermore, it is coated high transmission at 1064 ($T > 95\%$) and high reflection (HR) at 1573 nm ($R > 99.8\%$) on one side, serving as a cavity mirror (M2) for the OPO, and AR coated at both 1064 nm and 1573 nm on the other side. As the input mirror, M1 is high transmission at 808 nm on both sides and high reflection at 1064 nm on the concave side, with a radius of the curvature of 50 mm. As the cavity mirror for both the fundamental and OPO cavities, M3 is HR coated at 1064 nm ($R >$ 99.8%) and partly reflection at 1573 nm ($R = 86\%$) on one side, and high transmission at the two waves on the other side. Since the KTP is placed very close to M3, the OPO cavity, formed by M2 and M3, is approximately as long as the nonlinear crystal. In addition, several thermoelectric coolers are used in this setup to thermally stabilize the laser rod, Cr:YAG, and KTP crystal.

3. EXPERIMENTAL RESULTS AND DISCUSSION

The overall physical cavity length of the lasing source is designed to be approximately 57 mm to optimize the mode-to-pump ratio. And, in order to increase the parametric conversion efficiency, the y axis of the KTP is placed so that it is exactly parallel to the polarization direction of the fundamental wave. Note that our OPO is single resonant at the signal wave (1.57 μm). On the one hand, the output coupler is coated to be only high reflected at the signal and fundamental wave; on the other, absorption in the KTP crystal for a wavelength longer than 3.1 μm, is significantly high, which, to a great degree, attenuates the idler wave (3.28 μm) [10]. Figure 2 shows the spectrum for the signal, recorded by an AQ 6317B Spectrum Analyzer, with a center wavelength of 1573.3 nm.

The average output power of 1573 nm, as a function of incident pump power, is depicted in Fig. 3. The observed OPO oscillation threshold, in terms of diode pump power, is about 2.6 W. Note that the parametric oscillation threshold and conversion efficiency significantly depend on the intracavity intensity and polarization of the pump. Thus, a relatively low diode pump threshold can be achieved by using a more highly focused and well polarized pump beam. As shown in Fig. 3, the output of the signal increases linearly until the diode pump power reaches 6.2 W, and the maximum output is about 110 mW at this point. When the pump power goes beyond 6.2 W, the impact of the thermal lens effect (TLE) in the laser rod become serious, resulting in the falloff of the signal output power. The most widely used formula to describe the TLE is expressed as [11]

$$f = \frac{K_c}{\xi I_{in}(dn/dT)} \frac{1}{1 - \exp(-\alpha l)}, \qquad (1)$$

where K_c is the thermal conductivity, and α and dn/dT are the absorption and the thermo-optic coefficient, respectively. In addition, ξ is the fractional thermal load and l is the crystal length. And, the absorbed pump intensity I_{in} can be defined by

$$I_{in} = \frac{P_{in}}{\pi \omega_p^2}. \qquad (2)$$

Here, ω_p and P_{in} are the pump beam waist and absorbed pump power, respectively. For a 1.0 at. % doped $Nd:YVO_4$ crystal, K_c = 5.4 W/mK, α = 14.8 cm^{-1}, $dn/dT = (4.7 \pm 0.6) \times 10^{-6}$/K, $\xi = 0.3$, and $l = 2$ mm. Furthermore, at the critical absorbed diode pump power of 6.2 W, pump intensity I_{in} = 4.93 kW/cm^2. Based on these parameters and Eq. (1), we finally obtained the thermal focal length $f = 72$ mm. However, the measured focal length, at the diode pump power of 6.2 W, is only 44 mm. The discrepancy could be interpreted as follows. On the one hand, owing to the TLE, as Song et al. indicated in [12], the value of the pump beam waist in the active medium should be smaller than that we used in the calculation, which will result in a higher pump intensity. On the other, the TLE in the Cr:YAG saturable absorber, which is an important factor in high power output [13], has been omitted. Furthermore, if the TLE is not properly treated, continuous pump heating will lead to crystal fracturing. The absorbed pump power at the fracture limit is given by [14]

$$P_{lim} = \frac{1}{\beta} \frac{4\pi\delta}{\xi}, \qquad (3)$$

where $\delta \propto K_c$ is the thermal shock parameter, which depends on the mechanical and thermal properties of the host material. And, $\beta = 20N_d$ (cm^{-1}) is the absorption coefficient of the $Nd:YVO_4$ crystal at 808 nm, where N_d is the Nd-dopant concentration in units of at %. Equation (3) shows that the thermal-induced fracture of the laser rod is greatly related to its thermal conductivity and dopant concentration. Since the active medium used in our experiment is a 3 × 3 × 2 mm^3, 1.0 at. % doped $Nd:YVO_4$ crystal, with the disadvantage of a small thermal conductivity (only half of that of Nd:YAG), we have to limit the diode pump power at 6.6 W to avoid crystal fracturing.

During the operation of the IOPO system, in addition to the signal wave, we also observed some faint green light (532 nm), which is caused by the SHG effect of the pump wave. Moreover, in order to detect the temporal shape of both the signal and pump pulse, a prism is used to disperse the signal, pump, and green light. Figure 4 shows the typical temporal profile of the signal and pump wave, detected by two fast InGaAs photodiodes, and recorded by a LeCroy 9361C Dual 300 MHz oscilloscope. In this figure, one can clearly see the buildup mechanism of the signal pulse and also the correlation dynamics between the laser and the OPO, which can be interpreted in the following way. On the first stage, after the Cr:YAG crystal is bleached, the intracavity pump intensity increases with the pump level. When the pump intensity is sufficiently high to exceed the OPO threshold, the parametric conversion process starts, resulting in the fast build up of the signal pulse and, simultaneously, the rapid decrease of the pump field. As mentioned previously, IOPO acts as a cavity dumper to extract the pump energy to the signal pulses. If the stored energy is fully extracted, one single pulse is generated, and if not, a multipulsing phenomenon will emerge, as is shown in Fig. 4. A multipulsing situation of the IOPO is undesirable and should be avoided in practical use. One way to suppress it is to optimize the reflectivity at the signal wave of the output coupler [15].

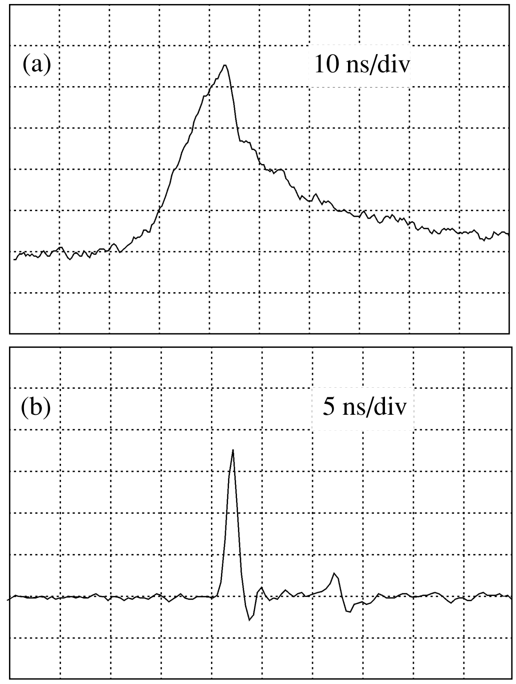

Fig. 4. Temporal profile of the fundamental wave after the OPO begins to oscillate. (b): Typical temporal shape of the signal pulses, with a pulse width of 1.3 ns.

In the experiment, the typical width of the fundamental pulse, before the OPO oscillation, was about 22 ns. At a incident diode pump power of 6.2 W and pulse repetition rate of 13 kHz, we get a minimum signal pulse duration of around 1.3 ns, which is about 17 times shorter than that of the pump. To the best of our knowledge, this is the most efficient pulse-shortening mechanism. Furthermore, the roundtrip time of the IOPO system is about 0.5 ns, which indicates that the pump field is depleted in approximately 2.5 roundtrips, suggesting, once more, the cavity dumping characteristic of the IOPO. In addition, at a diode pump power of 6.2 W, we also obtain a maximum pulse energy of 8.5 μJ at 1573 nm.

4. CONCLUSIONS

In conclusion, we have accomplished a compact eye-safe IOPO, driven by a diode end-pumped passively Q-switched $Nd:YVO_4/Cr:YAG$ laser. Owing to the efficient pulse-shortening mechanism, a signal pulse width as short as 1.3 ns is obtained, exhibiting a compressing factor of 17 with respect to the fundamental pulse. Experimental results show that such a kind of IOPO system is a promising eye-safe laser source in terms of practical application and commercialization. By reducing the influence of the thermal lens (e.g., to lower the dopant concentration and increase the length of the active medium), we expect a watt-level signal average output under the same pump scheme.

REFERENCES

1. L. R. Marshall, A. Kaz, and R. L. Burnham, Proc. SPIE **1627**, 262 (1992).
2. W. Zendzian, J. K. Jabczynski, J. Kwiatkowski, et al., Appl. Phys. B **80**, 329 (2005).
3. W. Zendzian, J. K. Jabczynski, and J. Kwiatkowski, Appl. Phys. B **76**, 355 (2003).
4. Y. F. Chen, Opt. Lett. **29**, 2632 (2004).
5. L. Fornasiero, S. Kuck, T. Jensen, et al., Appl. Phys. B **67**, 549 (1998).
6. E. V. Raevsky, P. L. Pavlovitch, and V. A. Konovalov, Proc. SPIE **4630**, 75 (2002).
7. R. Dabu, A. Stratan, C. Fenic, et al., Opt. Eng. **40**, 455 (2001).
8. J. Liu and D. Kim, IEEE J. Quantum Electron. **35**, 1724 (1999).
9. X. Zhang, S. Zhao, Q. Wang, et al., IEEE J. Quantum Electron. **33**, 2286 (1997).
10. J. Miao, H. Tan, H. Bian, et al., Opt. Commun. **265**, 349 (2006).
11. M. E. Innocenzi, H. T. Yura, C. L. Fincher, et al., Appl. Phys. Lett. **56**, 1831 (1990).
12. F. Song, C. Zhang, X. Ding, et al., Appl. Phys. Lett. **81**, 2145 (2002).
13. J. Song, C. Li, and K. Ueda, Opt. Commun. **177**, 307 (2000).
14. Y. F. Chen, IEEE J. Quantum Electron. **35**, 234 (1999).
15. G. H. Xiao, M. Bass, and M. Acharekar, IEEE J. Quantum Electron. **34**, 2241 (1998).